RESEARCH ARTICLE
eISSN 2234-1757
Fish Aquat Sci. 2026;29(6):382-389
https://doi.org/10.47853/FAS.2026.e33
FAS Fisheries and Aquatic Sciences

3D-printed starfish $CaCO_3$/polycaprolactone scaffolds with enhanced *in vitro* osteogenesis for bone tissue engineering

Tae-Hee Kim[1, 2], Seung-Hee Moon[3], Fazlurrahman Khan[1, 2, 4, 5], Soo-Jin Heo[3, 6], Won-Kyo Jung[1, 2, 7], Seong-Yeong Heo[3, 6, *]

[1] *Research Center for Marine-Integrated Bionics Technology, Pukyong National University, Busan 48513, Korea*
[2] *Marine Integrated Biomedical Technology Center, The National Key Research Institutes in Universities, Pukyong National University, Busan 48513, Korea*
[3] *Jeju Bio Research Center, Korea Institute of Ocean Science and Technology (KIOST), Jeju 63349, Korea*
[4] *Ocean and Fisheries Development International Cooperation Institute, Pukyong National University, Busan 48513, Korea*
[5] *International Graduate Program of Fisheries Science, Pukyong National University, Busan 48513, Korea*
[6] *Department of Marine Technology & Convergence Engineering (Marine Biotechnology), University of Science and Technology (UST), Daejeon 34113, Korea*
[7] *Major of Biomedical Engineering, Division of Smart Healthcare, College of Information Technology and Convergence and New-senior Healthcare Innovation Center (BK21 Plus), Pukyong National University, Busan 48513, Korea*

Abstract

The development of marine-derived biomaterials has emerged as a promising approach for creating sustainable and biocompatible materials for tissue engineering. Marine organisms possess unique compositions and hierarchical structures that can inform next-generation scaffolds for bone regeneration. In this study, we developed a three-dimensional scaffold composed of polycaprolactone (PCL) and calcium carbonate (CC) derived from the marine organism *Crossaster papposus japonicus* (CCJ). Structural characterization using Fourier-transform infrared spectroscopy and X-ray diffraction confirmed that CCJ has high crystallinity and is chemically comparable to commercial CC. *In vitro* assays using MC3T3-E1 pre-osteoblasts demonstrated excellent biocompatibility, significantly increased alkaline phosphatase activity, and enhanced calcium deposition, indicating osteogenic differentiation. Integrating biodegradable PCL with marine-derived CCJ yielded a bio-functional scaffold with strong potential for bone tissue engineering. Overall, these findings highlight marine-integrated sustainable biomaterials as alternatives for the designing cost-effective and environmentally responsible scaffolds for guided bone regeneration.

Keywords: Calcium carbonate, Starfish, 3D scaffold, Bone regeneration

Received: Nov 17, 2025 **Revised:** Jan 27, 2026 **Accepted:** Jan 28, 2026
***Corresponding author:** Seong-Yeong Heo
Jeju Bio Research Center, Korea Institute of Ocean Science and Technology (KIOST), Jeju 63349, Korea
Tel: +82-64-798-6011, **Fax:** +82-64-798-6011, **E-mail:** syheo@kiost.ac.kr

Introduction

Bone is a dynamic, highly vascularized tissue that undergoes continuous remodeling in response to mechanical and metabolic stimuli (Laubach et al., 2022). It comprises a calcified matrix-approximately 65% inorganic material, 25% organic material, and 10% water-together with cellular components (osteoblasts, osteoclasts, and osteocytes) and regulatory proteins such as osteocalcin, osteopontin, and osteoprotegerin (Kim et al., 2022; Laubach et al., 2022). Although bone has a remarkable regenerative capacity and can restore its original structure and function after minor injuries (e.g., fractures and small defects), critical-sized bone defects caused by trauma, tumor resection, infection, congenital malformation, or degenerative diseases exceed its intrinsic healing capacity and therefore require clinical intervention (Wang et al., 2023; Wang et al., 2021b; Yang et al., 2023).

Traditional treatment strategies, including autografts, allografts, and xenografts, remain the standard of care; however, they present significant limitations, such as donor-site morbidity, immune rejection, infection risk, and limited tissue availability (Wang et al., 2022b; Zhang et al., 2023). Against this backdrop, bone tissue engineering has emerged as a promising alternative that seeks to develop bioinspired scaffolds capable of recapitulating the structural, mechanical, and biological features of native bone (Li et al., 2024; Li et al., 2022; Shen et al., 2023). An ideal scaffold should not only promote the expression of biomarkers (e.g., osteocalcin, osteopontin, and osteoprotegerin) but also support mineralization, which is a critical for restoring the architecture and function of damaged bone (Wang et al., 2021b; Zhou et al., 2021).

Recent advances in fabrication techniques, including electrospinning and three-dimensional (3D) printing, have enabled the development of biomimetic scaffolds that more closely resemble the extracellular matrix and support both osteogenic differentiation and angiogenesis (Banimohamad-Shotorbani et al., 2021; Zhang et al., 2023; Zhou et al., 2021). In addition, incorporating functional agents such as bioceramics, anti-inflammatory drugs, and anti-bacterial drugs has further improved scaffold performance by enhancing osteogenic marker expression, promoting mineralization, and even supporting neuroregeneration (Heo et al., 2019; Kim et al., 2024; Shen et al., 2023).

Biomaterials play a central role in contemporary regenerative strategies, serving as scaffolds, drug carriers, and bioactive matrices that interact with biological systems to promote tissue repair and regeneration (Hosseini et al., 2023; Kim et al., 2023; Kurdi & M-Ridha, 2023). These materials are engineered to replace or support damaged tissues, facilitate healing, and ultimately restore function (Oleksy et al., 2023; Zheng et al., 2023). In particular, biomaterials for bone regeneration are designed to mimic the structural and mechanical characteristics of natural bone, thereby supporting the repair of defects arising from trauma, disease, or congenital conditions (Szwed-Georgiou et al., 2023; Xing et al., 2023). Their capacity to support cellular activities, promote osteogenesis, and undergo controlled degradation makes them essential for developing effective bone-regenerative therapies.

Polycaprolactone (PCL) is a synthetic, biodegradable polymer that has attracted considerable attention in tissue engineering, especially for bone regeneration (Javkhlan et al., 2024; Oh et al., 2021). This semi-crystalline aliphatic polyester has been approved by the United States Food and Drug Administration for various biomedical applications owing to its favorable biocompatibility, mechanical integrity, and slow degradation rate (Kim et al., 2023; Wang et al., 2022a). However, PCL is intrinsically hydrophobic, which limits cell adhesion and bioactivity due to poor surface wettability. These drawbacks can be mitigated by incorporating bioactive components such as calcium carbonate ($CaCO_3$, CC), tricalcium phosphate, or marine-derived collagen to enhance osteoconductivity and cell-material interactions (Erdemli et al., 2024; Ferreira et al., 2012).

CC is a biofunctional material widely investigated for bone regeneration because of its biocompatibility, biodegradability, and osteoconductivity (Erdemli et al., 2024; Reyna-Urrutia et al., 2023; Wang et al., 2021a). By providing an inorganic phase analogous to that of native bone, CC can improve osteoblast attachment and activity. In addition, compared with hydroxyapatite, CC often exhibits more favorable biodegradability that can better match the pace of physiological remodeling (Jiang et al., 2023; Liu & Wang, 2023; Xu et al., 2021). Accordingly, CC-containing scaffolds have shown promising outcomes in supporting bone formation and regeneration (Erdemli et al., 2024; Liu & Wang, 2023; Xu et al., 2021). Nevertheless, commercially available CC is typically produced via synthesis and resource-intensive processing, raising concerns regarding cost and environmental sustainability.

To address these limitations, we explored an alternative CC source derived from the marine organism *Crossaster papposus*

japonicus, an abundant yet ecological underutilized species. CC extracted from *C. papposus japonicus* (CCJ) can be obtained as a by-product of existing from existing marine resource-utilization activities, thereby avoiding the need for dedicated harvesting. Although collection and freeze-drying still incur processing costs, the absence of raw-material procurement costs and the relative simplicity of the extraction procedure may reduce overall expenses compared to conventional chemically synthesized CC (c-CC). Moreover, CCJ may achieve comparable or improved biological performance at lower loading levels than c-CC, which could further enhance cost efficiency. Importantly, valorizing a marine by-product aligns with sustainability goals and supports the development of cost-effective, high-performance scaffolds for clinical translation.

Therefore, the primary objective of this study was to extract and comprehensively characterize CCJ and to fabricate a PCL-based composite scaffold using 3D printing. We further aimed to systematically evaluate the physicochemical properties and biological performance of the resulting PCL/CCJ scaffold and to assess its feasibility as a cost-effective, bioactive, and sustainable biomaterial platform for guided bone regeneration.

Materials and Methods

Materials

C. papposus japonicus was collected from the deep-sea floor (depth range: 300–1,000 m) near Wangdol-cho, located in the southwestern East Sea, during a trawl survey conducted by the National Institute of Fisheries Science in June 2017. Ethanol, sodium hypochlorite, sodium hydroxide, and sodium phosphate were purchased from Ducksan Chemical (Ansan, Korea). α-Minimum Eagle's Medium (α-MEM), fetal bovine serum (FBS), and penicillin/streptomycin/amphotericin were obtained from Gibco (NY, USA). 1-Step™ p-NPP, 3-(4,5-dimethylthiazol-2-yl)-2,5-diphenyltetrazolium bromide (MTT), dimethyl sulfoxide (DMSO), PCL, Alizarin Red S, ascorbic acid, β-glycerophosphate, and cetylpyridinium chloride were purchased from Sigma-Aldrich (St. Louis, MO, USA). All other chemicals and reagents were commercially available.

CC from *C. papposus japonicus* (CCJ) extraction

CCJ was extracted following a previously reported method with minor modifications (Kurdi & M-Ridha, 2023). Briefly, *C. papposus japonicus* was washed with tap water, rinsed with distilled water, and frozen at –80℃. The frozen samples were lyophilized and homogenized into a fine powder. A total of 100 g of powder was treated with 2.5 L of 70% ethanol to remove soluble impurities. The mixture was filtered through filter paper (GE Healthcare, Chicago, IL, USA), and the residue was collected. The residue was then treated with sodium hypochlorite and stirred for 12 h to eliminate remaining organic components, followed by filtration. Subsequently, the residue was treated with sodium phosphate for 2 h to induce CCJ precipitation. The suspension was centrifuged (25,000×g, 3 mins), and the resulting pellet was washed thoroughly with distilled water. The final CCJ powder was dried in a drying oven to remove residual moisture and stored at –80℃ until use.

Characterization of the CC from *C. papposus japonicus* (CCJ)

To identify the functional groups present in CCJ and c-CC, Fourier transform infrared (FT-IR) spectra were acquired using an FT-IR spectrometer (JASCO, Tokyo, Japan). Samples were prepared using the conventional KBr pellet method. Spectra were collected over 650–4,000 cm^{-1} at a resolution of 4 cm^{-1} with 30 scans.

X-ray diffraction (XRD) analysis was performed using an XRD diffractometer (X'Pert3 Powder, Malvern Panalytical, Almelo, Netherlands) with Cu-Kα radiation. Diffraction patterns were recorded over a 2θ range of 5° to 90° at a scanning rate of 2.4°/min to assess the crystalline structure and phase purity of CCJ and c-CC.

Cytotoxicity and effect on *in vitro* differentiation of the CC from *C. papposus japonicus* (CCJ)

MC3T3-E1 pre-osteoblasts were obtained from the American Type Culture Collection (Rockville, MD, USA) and cultured in α-MEM supplemented with 10% FBS and penicillin/streptomycin/amphotericin. Cells were maintained at 37℃ in a humidified incubator with 5% CO_2 and subcultured every 3 days.

For cytotoxicity testing, MC3T3-E1 pre-osteoblasts were seeded in 24-well plates at a density of 1×10^5 cells/well. After 24 h, the cells were treated with CCJ at various concentrations (0–200 μg/mL in α-MEM) and incubated for 2 and 4 days. Cell viability was determined using an MTT assay. Briefly, 100 μL of MTT solution (1 mg/mL in PBS) was added to each well and incubated for 2 h at 37℃. Formazan crystals were dissolved in DMSO, and absorbance was measured at 540 nm using a microplate reader.

For alkaline phosphatase (ALP) activity, 100 μL of 1-Step™ p-NPP reagent was added to each well after 7 days of incubation and allowed to react for 30 min at RT. The reaction was terminated by adding 2 N NaOH, and absorbance was measured at 405 nm.

https://doi.org/10.47853/FAS.2026.e33

Fabrication of the osteogenic scaffolds

A three-axis robotic plotting system (EZ-ROBO-5GX ST2520, Iwashita Engineering, Kitakyushu, Japan), equipped with a dispenser was used to fabricate scaffolds as previously described (Heo et al, 2019; Kim et al., 2022). As shown in Fig. 1, PCL pellets were premixed with either c-CC or CCJ powder (1% w/w each), and the blended mixtures were melted in a heating barrel to obtain composite melts. The melts were extruded through a 400 μm heated nozzle at a constant pressure of 500 ± 25 kPa and a dispensing speed of 0.2 mm/s. The molten materials were deposited in a layer-by-layer manner to produce 3D scaffolds with uniform pore architecture. Each scaffold was fabricated at a size of 2 × 2 cm and subsequently trimmed for further experiments.

In vitro osteogenic effect of the fabricated scaffolds on MC3T3-E1

Calcium deposition was assessed by Alizarin Red S staining. Prior to cell seeding, scaffolds were sterilized with 70% ethanol and exposed to UV light for 30 min. MC3T3-E1 cells were seeded onto the scaffolds (0.5 × 0.5 mm) at a density of 1×10^5 cells/scaffold. Cells were cultured in osteogenic differentiation medium supplemented with 50 μg/mL ascorbic acid and 10 mM β-glycerophosphate, with medium changes every 2 days. After 7 and 14 days, cells were fixed with cold 70% ethanol and stained with 40 mM Alizarin Red S (pH 4.2) for 30 min at RT. Samples were then washed three times to remove excess stain. For quantification, the stained calcium deposits were eluted with cetylpyridinium chloride, and absorbance was measured at 562 nm using a microplate reader.

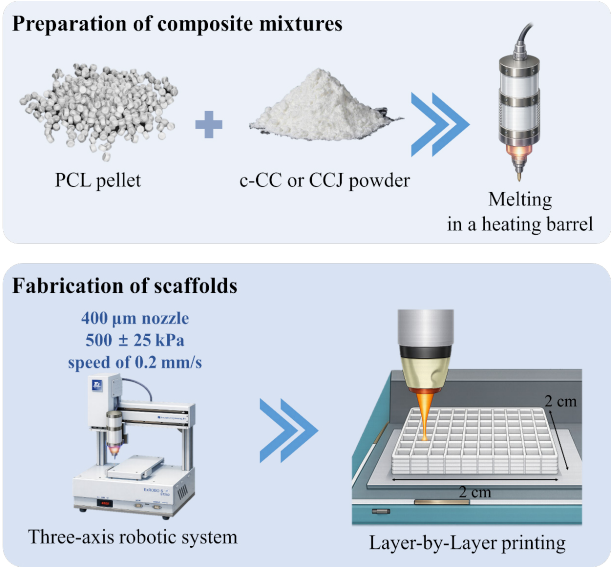

Fig. 1. Schematic representation of the fabrication process for PCL, PCL/c-CC, and PCL/CCJ scaffolds. PCL, polycaprolactone; c-CC, chemically synthesized calcium carbonate; CCJ, *Crossaster papposus japonicus*. This figure was created using AI-assisted image generation and subsequently edited by the authors.

Statistical analysis

All data are presented as the mean ± standard deviation from at least three independent experiments. Statistical significance was evaluated using one-way analysis of variance (ANOVA) followed by Duncan's multiple range test. Analyses were performed using SPSS Statistics (version 12.0; Chicago, IL, USA). Statistical significance was defined as $^{*}p < 0.05$ and $^{**}p < 0.10$.

Results and Discussion

Characteristics of CC from *C. papposus japonicus* (CCJ)

CCJ was successfully extracted using sodium hypochlorite pre-treatment followed by sodium phosphate treatment, and its characteristics were evaluated by FT-IR and XRD. The FT-IR spectra of c-CC and CCJ are shown in Fig. 2A. Both samples exhibited characteristic carbonate bands, including the ν_3 asymmetric stretching vibration of CO_3^{2-} at 1,400 cm^{-1} and the ν_4 in-plane bending vibration at 725 cm^{-1} (Naknonhan et al., 2025). In addition, peaks at 1,080 cm^{-1} and 874 cm^{-1} corresponded to carbonate vibrational modes (Rodriguez-Blanco et al., 2011). In c-CC, a broad band in the range of 2,850–3,050 cm^{-1} was observed and attributed to O-H stretching vibrations.

The XRD pattern of the CCJ (Fig. 2B) indicated a highly crystalline phase, with diffraction peaks consistent with calcite calcium carbonate (JCPDS card No. 01-072-1650) (Liu et al., 2018). No additional peaks beyond those assigned to $CaCO_3$ were detected, suggesting that CCJ exhibits a phase purity comparable to that of commercial c-CC. Collectively, these results confirm that CC was successfully extracted from CCJ and that its chemical features are comparable to those of c-CC, supporting CCJ as a potential biomaterial for bone regeneration applications.

Biological effect of CC from *C. papposus japonicus* (CCJ) on MC3T3-E1 cells

The cytotoxicity of CCJ was assessed using the MTT assay. MC3T3-E1 pre-osteoblasts were treated with CCJ (0–200 μg/

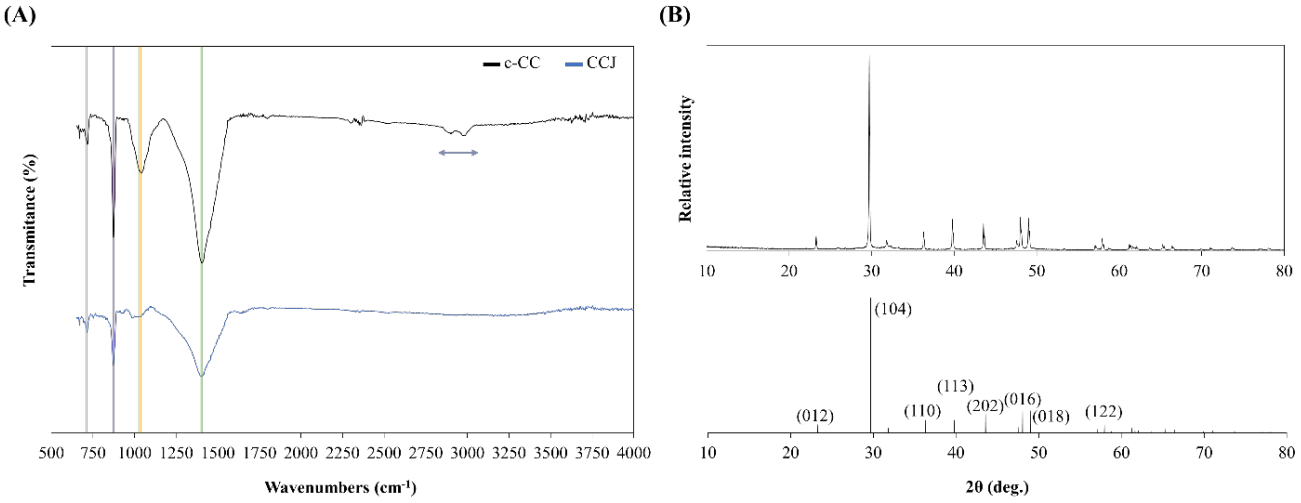

Fig. 2. Chemical analysis of CCJ. (A) FT-IR spectrum and (B) XRD pattern of CCJ. c-CC, chemically synthesized calcium carbonate; CCJ, *Crossaster papposus japonicus*; FT-IR, Fourier transform infrared; XRD, X-ray diffraction.

mL) for 2 and 4 days. As shown in Fig. 3A, CCJ did not reduced cell viability at any tested concentration, indicating no detectable cytotoxicity under these conditions.

Induction of osteogenic differentiation is an important criterion for bone-regeneration biomaterials. ALP, an early osteogenic marker, contribute to phosphate metabolism by catalyzing the hydrolysis of phosphomonoester bonds (Heo et al, 2019; Xu et al, 2021). Accordingly, the effect of CCJ on ALP activity was evaluated in MC3T3-E1 cells. As shown in Fig. 3B, treatment with 200 μg/mL CCJ for 7 days increased ALP activity relative to the untreated control, showing a statistical trend ($p < 0.1$). This elevation suggests the early initiation of osteoblast differentiation, potentially associated with increased calcium ion availability from CCJ (Amamoto et al., 2022; Assefa et al., 2022; Jeon et al., 2021).

Overall, these findings suggest that CCJ can support osteogenic responses, potentially by providing bioavailable calcium and enhancing cell-matrix interactions (Erdemli et al., 2024; Wang et al., 2021a). Moreover, the osteogenic performance of PCL/CCJ scaffolds may reflect synergistic effects between the osteoconductive CCJ phase and the mechanical stability provided by the PCL matrix, which together create a favorable microenvironment for osteogenic commitment (Kim et al., 2024; Oh et al., 2021).

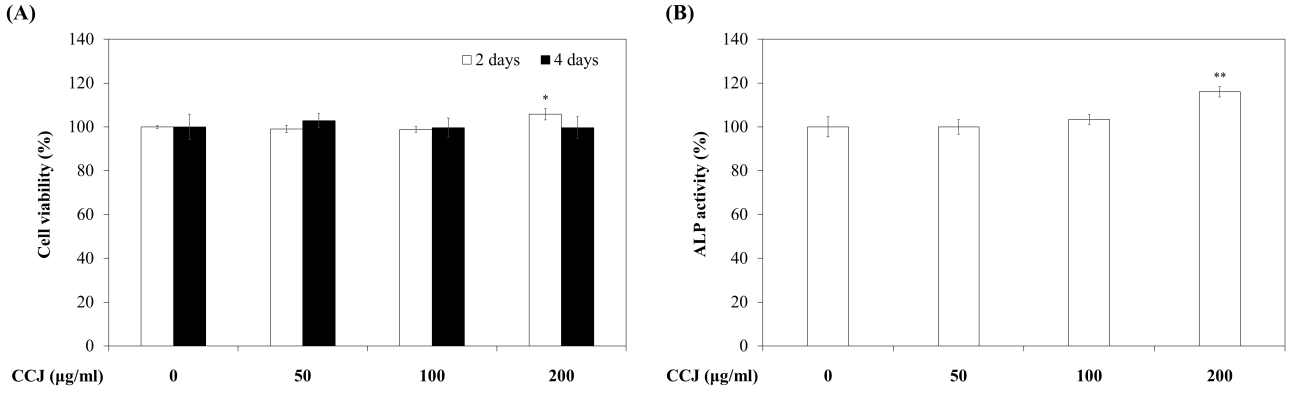

Fig. 3. Biological effects of CCJ on MC3T3-E1 cells. (A) Biocompatibility at 2 and 4 days, and (B) ALP activity of CCJ on MC3T3-E1 pre-osteoblasts at 7 days. $^{*}p < 0.05$ and $^{**}p < 0.10$ were considered statistically significant compared with the untreated group. CCJ, *Crossaster papposus japonicus*; ALP, alkaline phosphatase.

https://doi.org/10.47853/FAS.2026.e33

In vitro calcium deposition effect of polycaprolactone (PCL)/CC from *C. papposus japonicus* (CCJ) scaffolds

Mineralization is a key function of osteoblasts during bone regeneration (Ponzetti & Rucci, 2021). To evaluate mineralization *in vitro*, calcium deposition by MC3T3-E1 cells cultured on the fabricated scaffolds was assessed at 7 and 14 days using Alizarin Red S staining. As shown in Fig. 4, PCL/CCJ scaffolds enhanced calcium deposition compared with PCL and PCL/c-CC scaffolds, with deposition increasing over time. The PCL/CCJ group exhibited the highest mineralization at both time points.

These results indicate that PCL/CCJ scaffolds promotes extracellular matrix mineralization, likely due to the combined contributions of osteoconductive CCJ and the structural integrity provided by the PCL framework. The greater effect observed for CCJ relative to c-CC may be related to differences in bioceramic particle characteristics, such as particle size and morphology, which can influence osteogenic performance (Hayashi et al., 2020). Therefore, future studies will examine the impacts effects of particle size and related physicochemical parameters on osteogenic outcomes in greater detail. Collectively, these findings demonstrate the strong *in vitro* bone-regenerative potential of the PCL/CCJ scaffold.

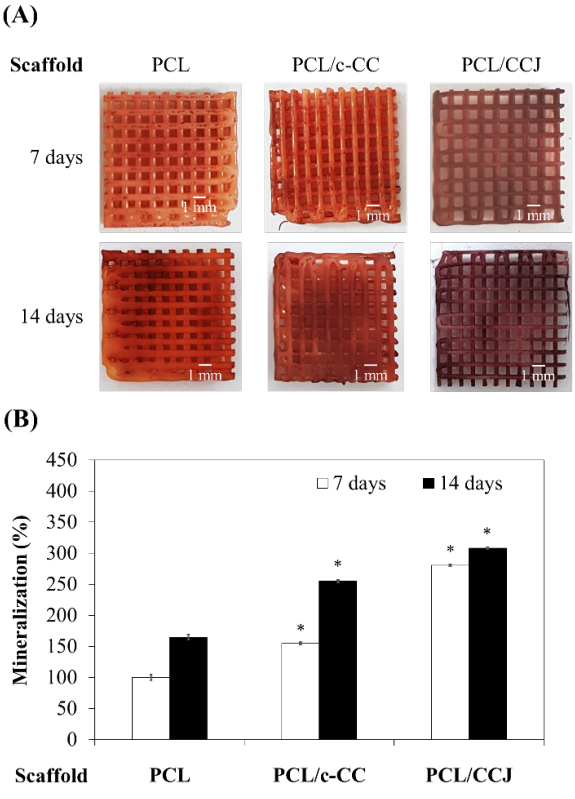

Fig. 4. Effect of fabricated scaffolds on mineralization assessed by Alizarin Red S staining. (A) Optical image and (B) quantification of mineralization in fabricated scaffolds. * $p < 0.05$ was considered statistically significant compared with the untreated group. PCL, polycaprolactone; c-CC, chemically synthesized calcium carbonate; CCJ, *Crossaster papposus japonicus*.

Conclusion

In this study, CC was successfully extracted from *C. papposus japonicus* and incorporated into a morphologically uniform PCL/CCJ scaffold. *In vitro* evaluation using MC3T3-E1 pre-osteoblasts showed that CCJ increased ALP activity without detectable cytotoxicity. Moreover, the PCL/CCJ scaffold significantly enhanced extracellular matrix mineralization *in vitro*. Collectively, these findings highlight the potential of marine-derived CCJ as a bioactive filler and support the PCL/CCJ scaffolds as a promising candidates for bone regeneration.

Competing interests

No potential conflict of interest relevant to this article was reported.

Funding sources

This research was supported by the Basic Science Research Program through the National Research Foundation of Korea (NRF) by the Ministry of Science and ICT (RS-2023-00212069, RS-2025-00519462).

Acknowledgements

Not applicable.

Availability of data and materials

Upon reasonable request, the datasets of this study can be available from the corresponding author.

Ethics approval and consent to participate

Not applicable.

ORCID

Tae-Hee Kim https://orcid.org/0000-0002-0988-0193
Seung-Hee Moon https://orcid.org/0009-0001-7564-4172
Fazlurrahman Khan https://orcid.org/0000-0002-4902-3188
Soo-Jin Heo https://orcid.org/0000-0003-2092-967X
Won-Kyo Jung https://orcid.org/0000-0002-1615-750X
Seong-Yeong Heo https://orcid.org/0009-0009-1348-663X

References

Amamoto S, Yoshiga D, Tabe S, Kokabu S, Fujii W, Hikiji H, et al. Zoledronate and lipopolysaccharide suppress osteoblast differentiation through downregulating phosphorylation of Smad in pre-osteoblastic MC3T3-E1 cells. J Oral Maxillofac Surg Med Pathol. 2022;34:472-9.

Assefa F, Kim JA, Lim J, Nam SH, Shin HI, Park EK. The neuropeptide spexin promotes the osteoblast differentiation of MC3T3-E1 cells via the MEK/ERK pathway and bone regeneration in a mouse calvarial defect model. Tissue Eng Regen Med. 2022;19:189-202.

Banimohamad-Shotorbani B, Rahmani Del Bakhshayesh A, Mehdipour A, Jarolmasjed S, Shafaei H. The efficiency of PCL/HAp electrospun nanofibers in bone regeneration: a review. J Med Eng Technol. 2021;45:511-31.

Erdemli Ö, Yilmaz B, Saran İG, Serin E. Sustainable biomaterials for tissue engineering: electrospun polycaprolactone fibers enriched with freshwater snail calcium carbonate and waste human hair keratin. Polym Int. 2024;73:833-43.

Ferreira AM, Gentile P, Chiono V, Ciardelli G. Collagen for bone tissue regeneration. Acta Biomater. 2012;8:3191-200.

Hayashi K, Munar ML, Ishikawa K. Effects of macropore size in carbonate apatite honeycomb scaffolds on bone regeneration. Mater Sci Eng C. 2020;111:110848.

Heo SY, Ko SC, Oh GW, Kim N, Choi IW, Park WS, et al. Fabrication and characterization of the 3D-printed polycaprolactone/fish bone extract scaffolds for bone tissue regeneration. J Biomed Mater Res B Appl Biomater. 2019;107:1937-44.

Hosseini FS, Abedini AA, Chen F, Whitfield T, Ude CC, Laurencin CT. Oxygen-generating biomaterials for translational bone regenerative engineering. ACS Appl Mater Interfaces. 2023;15:50721-41.

Javkhlan Z, Hsu SH, Chen RS, Chen MH. 3D-printed polycaprolactone scaffolds coated with beta tricalcium phosphate for bone regeneration. J Formos Med Assoc. 2024;123:71-7.

Jeon S, Lee JH, Jang HJ, Lee YB, Kim B, Kang MS, et al. Spontaneously promoted osteogenic differentiation of MC3T3-E1 preosteoblasts on ultrathin layers of black phosphorus. Mater Sci Eng C. 2021;128:112309.

Jiang P, Hou R, Chen T, Bai L, Li J, Zhu S, et al. Enhanced degradation performance and promoted bone regeneration of novel $CaCO_3$-based hybrid coatings on magnesium alloy as bioresorbable orthopedic implants. Chem Eng J. 2023;467:143460.

Kim SC, Heo SY, Oh GW, Yi M, Jung WK. A 3D-printed polycaprolactone/marine collagen scaffold reinforced with carbonated hydroxyapatite from fish bones for bone regeneration. Mar Drugs. 2022;20:344.

Kim TH, Kim SC, Park WS, Choi IW, Kim HW, Kang HW, et al. PCL/gelatin nanofibers incorporated with starfish polydeoxyribonucleotides for potential wound healing applications. Mater Des. 2023;229:111912.

Kim TH, Oh GW, Heo SY, Heo SJ, Kim YM, Lee DS, et al. 3D-printed polycaprolactone/collagen/alginate scaffold incorporating phlorotannin for bone tissue regeneration: assessment of sub-chronic toxicity. Int J Biol Macromol. 2024;282:137480.

Kurdi SS, M-Ridha MJ. The enhancement of sand properties by the use of plant-derived urease-induced calcium carbonate precipitation. Afr J Biol Sci. 2023;5:23-44.

Laubach M, Suresh S, Herath B, Wille ML, Delbrück H, Alabdulrahman H, et al. Clinical translation of a patient-specific scaffold-guided bone regeneration concept in four cases with large long bone defects. J Orthop Transl. 2022;34:73-84.

Li Z, Li S, Gao C, Liu J, Qu H, Yang J, et al. Continuous manufacturing of bioinspired bone-periosteum integrated scaffold to promote bone regeneration. Adv Funct Mater. 2024;34:2403235.

Li Z, Li S, Yang J, Ha Y, Zhang Q, Zhou X, et al. 3D bioprinted gelatin/gellan gum-based scaffold with double-crosslinking network for vascularized bone regeneration. Carbohydr Polym. 2022;290:119469.

Liu M, Kang M, Chen K, Mou Y, Sun R. Synthesis and luminescent properties of $CaCO_3$: Eu^{3+}@SiO_2 phosphors with core–shell structure. Appl Phys A. 2018;124:249.

Liu X, Wang Z. Chitosan-calcium carbonate scaffold with high mineral content and hierarchical structure for bone regeneration. Smart Mater Med. 2023;4:552-61.

Naknonhan S, Amnuaypanich S, Randorn C, Tanthanuch W, Amnuaypanich S. Pivotal role of $CaCO_3$ in Ca/ZnO photocatalyst for promoting the degradation of trichlorophenol. J Environ Chem Eng. 2025;13:115501.

Oh GW, Nguyen VT, Heo SY, Ko SC, Kim CS, Park WS, et al. 3D PCL/fish collagen composite scaffolds incorporating osteogenic abalone protein hydrolysates for bone regeneration application: *in vitro* and *in vivo* studies. J

https://doi.org/10.47853/FAS.2026.e33

Biomater Sci Polym Ed. 2021;32:355-71.

Oleksy M, Dynarowicz K, Aebisher D. Advances in biodegradable polymers and biomaterials for medical applications: a review. Molecules. 2023;28:6213.

Ponzetti M, Rucci N. Osteoblast differentiation and signaling: established concepts and emerging topics. Int J Mol Sci. 2021;22:6651.

Reyna-Urrutia VA, Rosales-Ibáñez R, González-González AM, Estevez M, Rodríguez-Martínez JJ, González-Reyna M. Biological activity of a chitosan-carboxymethylcellulose-zinc oxide and calcium carbonate in 3D scaffolds stabilized by physical links for bone tissue engineering. J Biomater Appl. 2023;37:1776-88.

Rodriguez-Blanco JD, Shaw S, Benning LG. The kinetics and mechanisms of amorphous calcium carbonate (ACC) crystallization to calcite, viavaterite. Nanoscale. 2011;3:265-71.

Shen M, Li Y, Lu F, Gou Y, Zhong C, He S, et al. Bioceramic scaffolds with triply periodic minimal surface architectures guide early-stage bone regeneration. Bioact Mater. 2023;25:374-86.

Szwed-Georgiou A, Płociński P, Kupikowska-Stobba B, Urbaniak MM, Rusek-Wala P, Szustakiewicz K, et al. Bioactive materials for bone regeneration: biomolecules and delivery systems. ACS Biomater Sci Eng. 2023;9:5222-54.

Wang S, Gu R, Wang F, Zhao X, Yang F, Xu Y, et al. 3D-Printed PCL/Zn scaffolds for bone regeneration with a dose-dependent effect on osteogenesis and osteoclastogenesis. Mater Today Bio. 2022a;13:100202.

Wang T, Zheng J, Hu T, Zhang H, Fu K, Yin R, et al. Three-dimensional printing of calcium carbonate/hydroxyapatite scaffolds at low temperature for bone tissue engineering. 3D Print Addit Manuf. 2021a;8:1-13.

Wang W, Wei J, Lei D, Wang S, Zhang B, Shang S, et al. 3D printing of lithium osteogenic bioactive composite scaffold for enhanced bone regeneration. Compos B Eng. 2023;256:110641.

Wang Y, Wang J, Gao R, Liu X, Feng Z, Zhang C, et al. Biomimetic glycopeptide hydrogel coated PCL/nHA scaffold for enhanced cranial bone regeneration via macrophage M2 polarization-induced osteo-immunomodulation. Biomaterials. 2022b;285:121538.

Wang Z, Wang Y, Yan J, Zhang K, Lin F, Xiang L, et al. Pharmaceutical electrospinning and 3D printing scaffold design for bone regeneration. Adv Drug Deliv Rev. 2021b;174:504-34.

Xing Y, Qiu L, Liu D, Dai S, Sheu CL. The role of smart polymeric biomaterials in bone regeneration: a review. Front Bioeng Biotechnol. 2023;11:1240861.

Xu W, Zhao R, Wu T, Li G, Wei K, Wang L. Biodegradable calcium carbonate/mesoporous silica/poly(lactic-glycolic acid) microspheres scaffolds with osteogenesis ability for bone regeneration. RSC Adv. 2021;11:5055-64.

Yang L, Fan L, Lin X, Yu Y, Zhao Y. Pearl powder hybrid bioactive scaffolds from microfluidic 3D printing for bone regeneration. Adv Sci. 2023;10:2304190.

Zhang X, Li Q, Li L, Ouyang J, Wang T, Chen J, et al. Bioinspired mild photothermal effect-reinforced multifunctional fiber scaffolds promote bone regeneration. ACS Nano. 2023;17:6466-79.

Zheng M, Wang X, Chen Y, Yue O, Bai Z, Cui B, et al. A review of recent progress on collagen-based biomaterials. Adv Healthc Mater. 2023;12:2202042.

Zhou X, Zhou G, Junka R, Chang N, Anwar A, Wang H, et al. Fabrication of polylactic acid (PLA)-based porous scaffold through the combination of traditional bio-fabrication and 3D printing technology for bone regeneration. Colloids Surf B Biointerfaces. 2021;197:111420.